Heliyon 10 (2024) e30446

Contents lists available at ScienceDirect

Heliyon

journal homepage: www.cell.com/heliyon

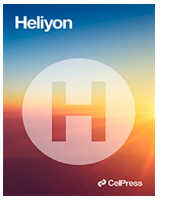

Research article

Prognostic value and immunological function of cuproptosis-related genes in lung adenocarcinoma

Liming Zhang [a,b], Shaoqiang Wang [c], Lina Wang [a,*]

[a] Medical Research Center, Affiliated Hospital of Jining Medical University, Jining Medical University, Jining, China
[b] Department of Thoracic Surgery, Weifang Second People's Hospital, Weifang, China
[c] Department of Thoracic Surgery, Weifang People's Hospital, Weifang Medical University, Weifang, China

ARTICLE INFO

Keywords:
Lung adenocarcinoma (LUAD)
Cuproptosis-related genes (CRGs)
Prognostic biomarker
Immunological function
Bioinformatics analysis

ABSTRACT

Background: Lung cancer is one of the malignant tumors with the highest morbidity and fatality rates worldwide. The overall survival (OS) of lung adenocarcinoma (LUAD) is poor. Cuproptosis is a copper-triggered modality of mitochondrial cell death, however, its contribution to the emergence of lung cancer is unknown. The clinical implication and immunological function of cuproptosis-related genes (CRGs) in LUAD has yet to be established.
Methods: TCGA, HPA, GEPIA, Kaplan-Meier, TIMER and CancerSEA database were used to explore the prognostic value and biological function of CRGs in LUAD.
Results: CRGs are primarily involved in copper ion transport, the citrate cycle (TCA cycle) and central carbon metabolism in LUAD. The mRNA expression of COA6, UBE2D1, DLAT, SLC25A3, and DBH was significantly increased. The expression of COA6, DLAT, SLC25A3, DBH, and LOXL2 were all strongly associated with the clinicopathological stages in LUAD. Moreover, high expression of COA6, UBE2D1, DLAT, SLC25A3 and LOXL2 was related to poor OS. The expression of SLC25A3 and LOXL2 showed different association with immune cell infiltration. The single cell sequencing demonstrated that CRGs play important roles in the regulation of DNA damage response, inflammation and metastasis in LUAD.
Conclusions: In summary, this study comprehensively uncovered that CRGs could be identified as potential prognostic and immunological biomarkers in LUAD. Our current research could provide a solid theoretical basis for LUAD survival research and clinical decision-making.

1. Introduction

Almost 1.3 million people worldwide die from lung cancer each year, accounting for about 18 % of all cancer deaths [1]. Lung cancer is one of the top causes of cancer deaths globally. It is mainly categorized into non-small-cell lung cancer (NSCLC) and small-cell lung cancer (SCLC) based on the histological categories, with NSCLC serving as the predominant pathological type of lung cancer and LUAD being the major type of NSCLC. At the time of diagnosis, more than 70 % of lung cancer patients have localized or advanced disease [2]. Currently, lung cancer patients can receive treatment with surgery, chemotherapy, targeted therapy, immunotherapy, and other methods [3], which have greatly increased the survival rates. However, the majority of patients with advanced lung cancer still

* Corresponding author. Medical Research Center, Affiliated Hospital of Jining Medical University, 89 Guhuai Road, Jining 272029, Shandong Province, China.
E-mail address: wanglina_china@163.com (L. Wang).

https://doi.org/10.1016/j.heliyon.2024.e30446
Received 29 January 2024; Received in revised form 26 April 2024; Accepted 26 April 2024
Available online 27 April 2024

have considerably low OS. Thus, it is crucial to discover much more trustworthy and promising biomarkers of prognosis in lung cancer patients.

By giving or receiving electrons, copper, a common metal element with redox activity, takes part in several biological processes [4]. In addition, copper is a vital mineral ingredient for all living things, and cancer cells require more copper than healthy ones [5–8]. Studies have indicated that people with cancers, such as breast cancer, gastrointestinal cancer, oral cancer, and thyroid cancer, have higher copper concentrations in their tumors or serum [9]. Thus, copper may play a crucial role in the emergence and growth of malignancies. The idea of cuproptosis, a copper-triggered mode of mitochondrial cell death [10], was initially put forth by Tsvetkov et al., in 2022. It differs from other proven ways of cell death, including apoptosis, pyroptosis, ferroptosis, and others [11–13]. The production of iron-sulfur cluster proteins is downregulated as a result of copper's direct binding to the fatty parts of the TCA cycle, which causes the accumulation of fatty acylated proteins, produces protein toxic stress, and ultimately results in cell death.

In our present study, by using multiple bioinformatics methods, we discovered several genes associated with copper mortality. Meanwhile, we investigated the prognostic significance and immunological function of these genes in patients with LUAD. Moreover, the potential function of CRGs in the regulation of LUAD biological behaviors was explored by single cell sequencing.

2. Materials and methods

2.1. Data download

Download LUAD transcriptome data and GSE101929 dataset from TCGA database (https://portal.gdc.cancer.gov/) [14] and the GEO database (https://www.ncbi.nlm.nih.gov/geo/) [15]; TCGA database includes 501 tumor samples and 54 normal samples; GSE101929 includes 32 tumor samples and 34 normal samples.

2.2. Mutation analysis of CRGs

Use the R (v4.2.2) program BiocManager [16] and the maftools [17] package to analyze the LUAD mutation information from TCGA database.

2.3. Enrichment analysis of the CRGs

We used the clusterProfiler package [18] and the enrichplot package for GO and KEGG enrichment analysis, respectively. The Hs. eg. db package is used for ID conversion. We explored the biological functions in which CRGs are primarily involved and visualized by the Chiplot (https://www.chiplot.online/) website.

2.4. Expression of CRGs in LUAD

We used the reshape2 pack and ggpubr package to extract LUAD expression data from TCGA, statistically analyze and visualize the expression of CRGs in LUAD, compare the expression of CRGs in tumor tissues and paracancerous tissues, and verify the results by transcriptome data in GSE101929.

2.5. Human protein atlas database analysis

The human protein atlas (HPA) [19] database is a public database that employs transcriptomics and proteomics methods to analyze the mRNA and protein expression in various human tissues and organs. The protein levels of CRGs in LUAD and healthy tissues was examined by the HPA database.

2.6. Relationship between CRG expression and clinicopathological staging

GEPIA (http://gepia.cancer-pku.cn/index.html) [20] integrates gene expression profile data from TCGA and GTEx projects and provides a variety of data analysis and visualization functions. When searching the GEPIA database, open the URL, enter CRGs, select "Stage plot" in the "Expression DIY" module, and analyze the correlation between CRGs expression and clinical stage feature.

2.7. Prognostic value of CRGs in LUAD

Kaplan-Meier plotter (http://www.kmplot.com) [21] integrates chip data from GEO, TCGA, and other databases to provide prognostic information for a variety of cancers, including lung cancer. We utilized this database to analyze the correlation between the expression of CRGs and the prognosis of LUAD patients.

2.8. Relationship between CRG expression and immune infiltration

We used MCP-counter, ssGSEA and TIMER (https://cistrome.shinyapps.io/timer/) [22] to evaluate the correlation between CRGs expression and immune cell infiltration in LUAD.

2.9. Immune checkpoints analysis

The TCGA dataset provided the RNAseq data and associated clinical information for LUAD. The eight immune checkpoint genes CD274, CTLA4, HAVCR2, LAG3, PDCD1, PDCD1LG2, TIGIT, and SIGLEC15 were retrieved between high and low expression of SLC25A3, as well as high and low expression of LOXL2. The above results are visualized by the R software packages ggplot2 and pheatmap.

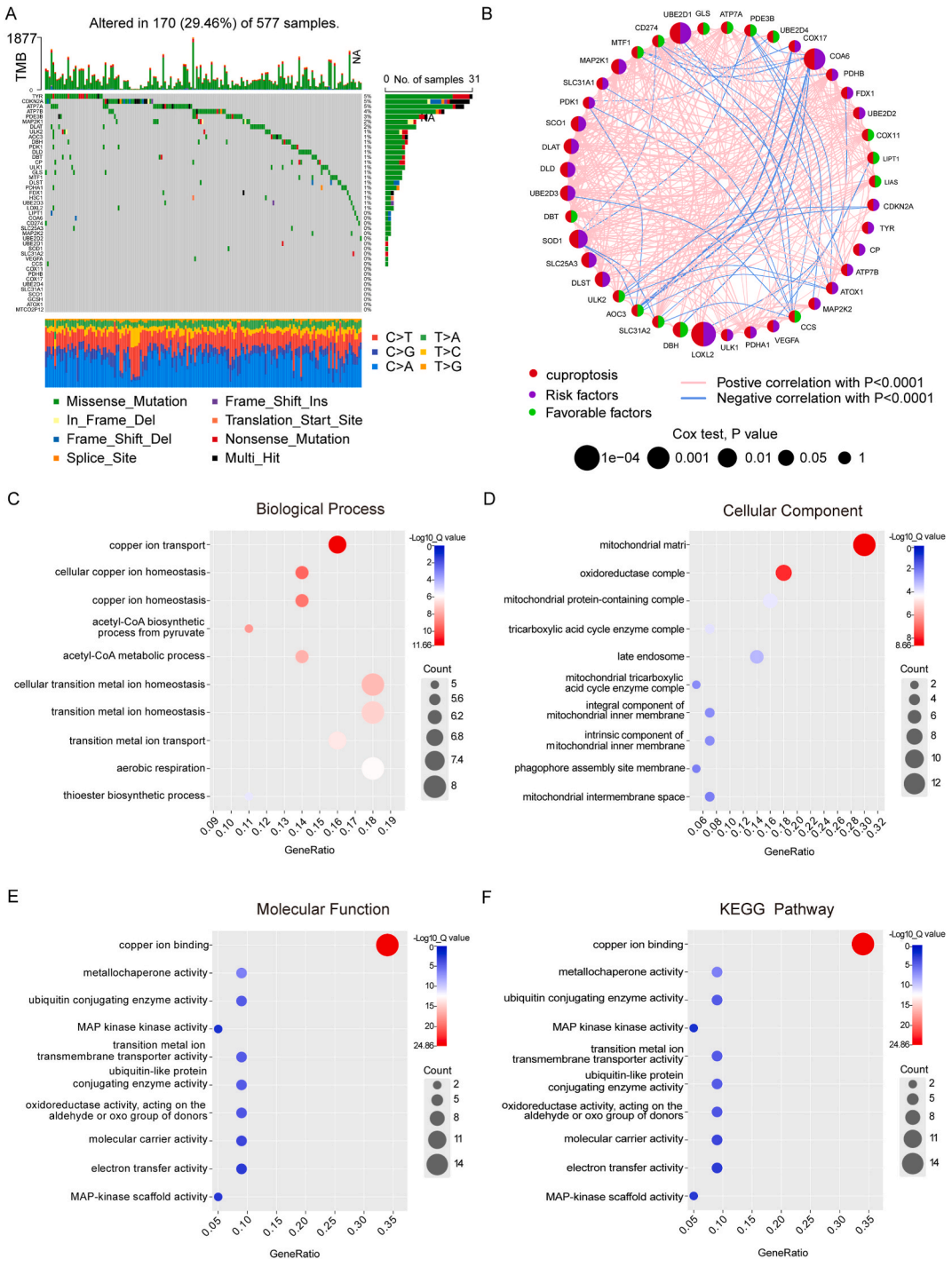

Fig. 1. Mutational and prognostic network map of CRGs with GO and KEGG in LUAD. (A) Mutational analysis of CRGs in LUAD. (B) Prognostic network map of CRGs in LUAD. (C) Biological process, (D) cellular component, (E) molecular function, and (F) KEGG pathways of CRGs in LUAD.

2.10. Drug sensitivity analysis

Download related drug data and gene expression data from the CellMiner website (https://discover.nci.nih.gov/cellminer/home.do). The impute package and the limma package were used for drug sensitivity analysis. Use the ggplot2 package for visualization.

2.11. Single cell sequencing

CancerSEA (http://biocc.hrbmu.edu.cn/CancerSEA/) [23] is a specialized single cell sequencing database, providing different functional status of cancer cells at the single cell level. The single-cell transcriptome sequencing is one of the most important techniques for analyzing the underlying function and molecular mechanism of candidate molecules at the single-cell level [24,25]. We analyzed the correlation between CRGs expression and different tumor biological function based on single cell sequencing data. T-SNE diagrams illustrated the expression profiles of CRGs at single cells of LUAD in TCGA samples.

2.12. Collection of human LUAD specimens

40 pairs of LUAD and non-cancerous tissues were collected from patients undergoing lung surgery in the Affiliated Hospital of Jining Medical University between Nov 2021 and Nov 2022. Before surgery, none of the patients had any prior history of cancer, and none had chemotherapy, radiation, or targeted treatment. Each patient signed an informed consent form. The ethics committee of the Affiliated Hospital of Jining Medical University examined and approved this work (Approval number 2021-11-C009).

2.13. RNA extraction and qRT-PCR analysis

TRIzol reagent was used to extract total cellular RNA (Invitrogen, USA). A commercial cDNA synthesis kit (SuperScript First-Strand Synthesis System, Thermo Fisher Scientific) was utilized to generate cDNAs by reverse transcription. The SYBR Green Assay Kit was used to detect the presence of mRNA (TAKARA, Japan). Using the Biosystems ViiA7 Sequence Detection System, the qRT-PCR procedure was carried out 3 times. Relevant primer sequences are listed in Supplementary Table S1.

2.14. Immunohistochemistry (IHC)

LUAD and paracancerous tissue samples were collected, and 3 mm of tumor sections were incubated with commercial rabbit polyclonal antibodies against COA6 (24209-1-AP, Proteintech), UBE2D1 (DF6715, Affinity), DLAT (13426-1-AP, Proteintech), SLC25A3 (10420-1-AP, Proteintech), DBH (DF7060, Affinity), LOXL2 (DF13442, Affinity) at 1/100 dilution overnight at 4^{o}C. Then, the sections were conjugated with horseradish peroxidase antibody at room temperature for 2 h, then substrates of the Envision system-HRP from the kit were added to incubate with stained slices as the manufacturer's protocol described. The signals were analyzed with a light microscope (Olympus 600, Tokyo, Japan). Control experiments without the primary antibody demonstrated that the signals observed were specific. We used imagePro-Plus (v6.0) software to analyze the immunohistochemical results, measure area and IOD values, process the results, and analyze the results quantitatively.

3. Results

3.1. Mutational and prognostic analysis of CRGs in LUAD

Initially, we analyzed and collated 41 cuproptosis-related genes (Supplementary Table S2) by reviewing the relevant literature [26–28]. After exploring the CRG mutation rate in LUAD, we obtained 170 of the 577 samples that showed gene alterations linked to cuproptosis, with a mutation frequency of 29.46 % (Fig. 1A). According to the CRGs network map created, the above 41 genes play significant roles in the determination of the prognosis of LUAD patients, respectively (Fig. 1B). Among all these genes, there are 26 risk factors, including UBE2D1, LOXL2, COA6, UBE2D3, DLAT, SOD1, SLC25A3, DLD, MAP2K, SCO1, DLST, PDK1, SLC31A, ULK1, PDHA1, VEGFA, MAP2K2, ATOX1, ATP7B, CP, TYR, CDKN2A, UBE2D2, FDX1, PDHB, and COX17, with 15 favorable factors, DBH, DBT, CCS, SLC31A2, MFT1, CD274, GLS, ATP7A, PDE3B, UBE2D4, ULK2, COX11, LIPT1, LIAS and AOC3.

3.2. GO and KEGG enrichment analyses of CRGs in LUAD

GO and KEGG analyses were used to explore the primary biological functions of CRGs in LUAD. Based on the GO results, the physiological roles of CRGs included copper ion transport, cellular copper ion homeostasis, the acetyl-CoA biosynthetic process from pyruvate, the acetyl-CoA metabolic process, which is mainly located in the mitochondrial matrix, mitochondrial protein-containing complex, tricarboxylic acid cycle enzyme complex, and so on (Fig. 1C and D). These genes perform molecular activities like copper ion binding, metallochaperone activity, and ubiquitin-conjugating enzyme activity (Fig. 1E). The KEGG pathway showed that CRGs were mostly involved in the TCA cycle, central carbon metabolism in cancer, the HIF-1 signaling pathway, carbon metabolism, and other processes (Fig. 1F).

3.3. Expression of CRG mRNA in LUAD

We downloaded and conducted analysis of the LUAD transcriptome data from TCGA database. The mRNA expression of LIAS, COX11, COA6, UBE2D4, GLS, UBE2D1, H3C1, PDK1, DLAT, DBT, SOD1, SLC25A3, CP, LOXL2, ULK1, GCSH, PDHA1, CCS, and MAP2K2, ATOX1, CDKN2A in LUAD tissues was higher than that in normal tissues, while FDX1, PDE3B, CD274, MTF1, SLC31A2, and DBH mRNA expression level showed significantly low in LUAD tissues, compared to the normal tissues (Fig. 2A). Meanwhile, the univariate analysis was performed to investigate the potential prognostic values of the above genes. The eight screened prognostic-related genes included seven potential risk genes (COA6, UBE2D1, DLAT, UBE2D3, SOD1, SLC25A3, LOXL2) and one potential protective gene (DBH) (Fig. 2B).

To further confirm the mRNA expression of CRGs in LUAD, the GSE101929 dataset and paired tissue data of TCGA were utilized for verification. The GSE101929 dataset showed that the mRNA expression of COA6, UBE2D1, DLAT, SLC25A3, and DBH was significantly elevated in LUAD, whereas UBE2D3, LOXL2 with low expression (Fig. 2C–J). Moreover, TCGA paired data demonstrated that COA6, UBE2D1, DLAT, SLC25A3 and LOXL2 were highly expressed in LUAD, while UBE2D3 was low expressed, with no significant difference in SOD1 and DBH expression (Supplementary Fig. 1).

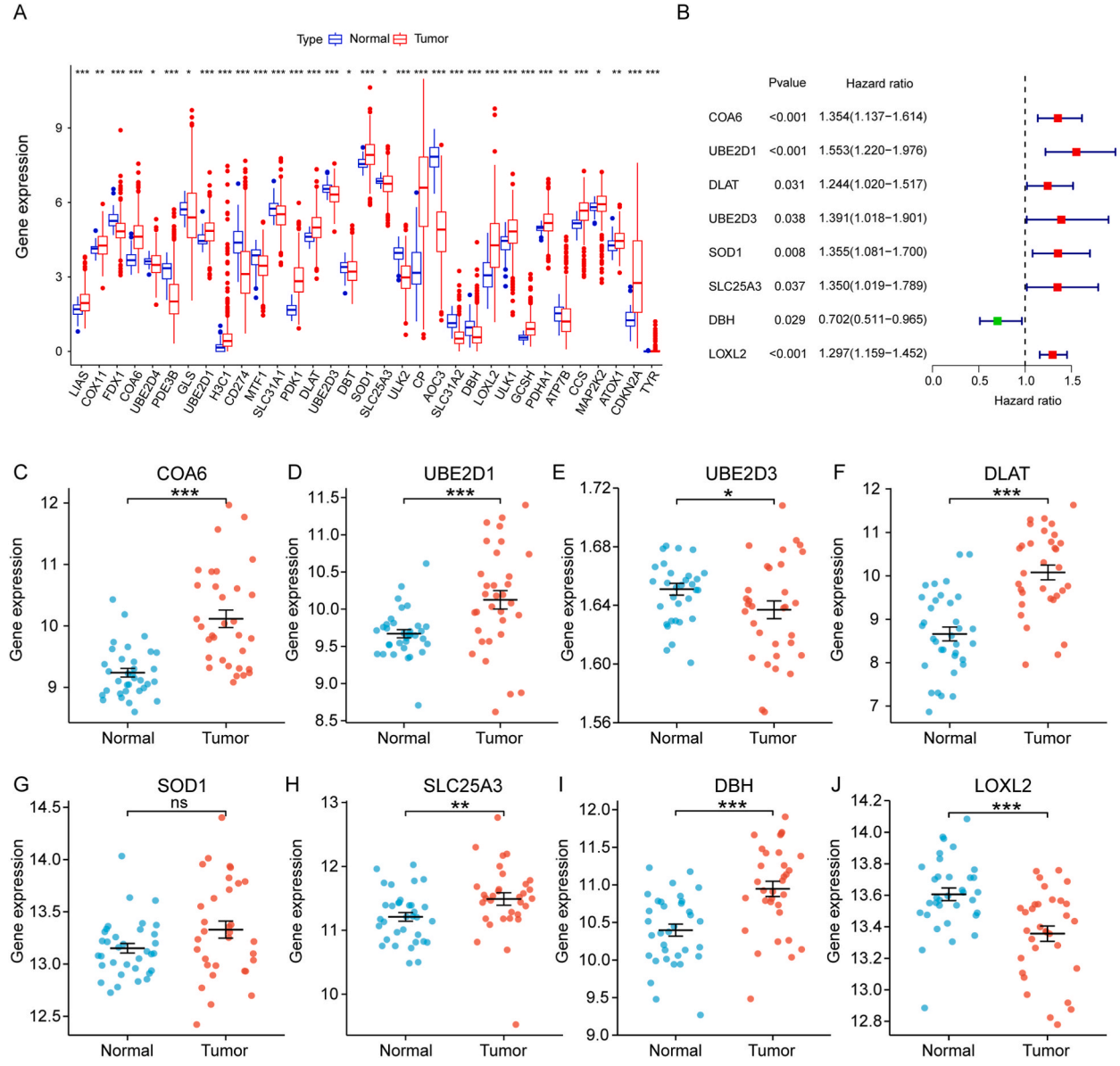

Fig. 2. The mRNA expression and Univariate analysis of CRGs in LUAD. (A) Expression of CRG mRNA in LUAD. (B) Univariate analysis of the eight CRGs in LUAD. (C–J) The mRNA expression of the eight CRGs in the GSE101929 dataset of LUAD.

3.4. CRG mRNA and protein expression in LUAD paired tissues

The freshly collected 40 paired tissues were used to perform qRT-PCR and immunohistochemistry (IHC) staining to explore the mRNA and protein expression of CRGs in LUAD. Similar to the aforementioned findings, COA6, UBE2D1, DLAT, SLC25A3 and LOXL2 showed higher expression in LUAD tissues, compared to the paracancerous tissues (Fig. 3A, B, D, F, H). UBE2D3 demonstrated decreased expression level, while SOD1 and DBH expression without significant difference (Fig. 3C–E, G).

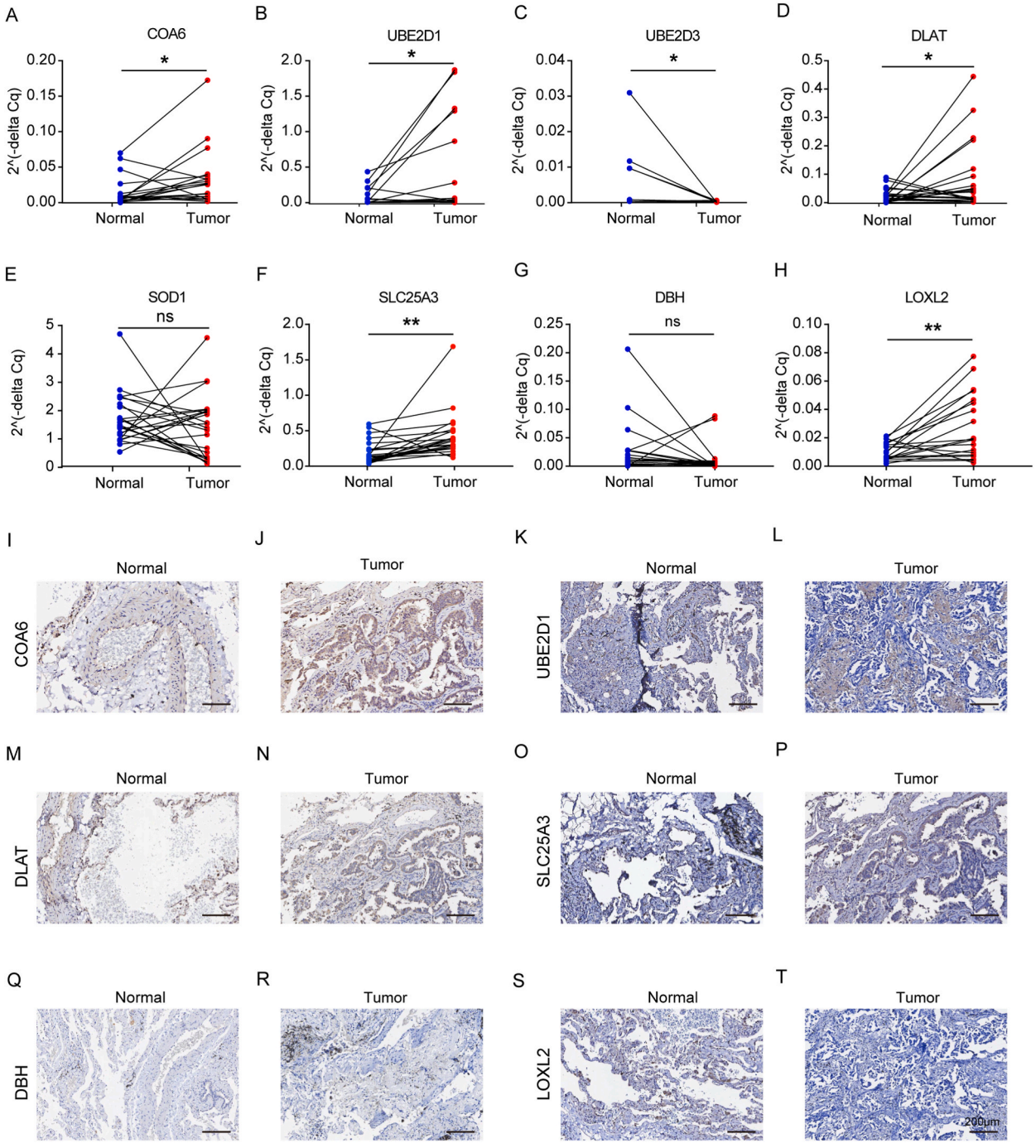

Fig. 3. CRG mRNA and protein expression in 40 LUAD paired tissues. The mRNA expression of (A) COA6 (B) UBE2D1 (C) UBE2D3 (D) DLAT (E) SOD1 (F) SLC25A3 (G) DBH, and (H) LOXL2 in LUAD paired tissues. The protein level of (I–J) COA6 (K–L) UBE2D1(M – N) DLAT (O–P) SLC25A3 (Q–R) DBH, and (S–T) LOXL2 in normal and LUAD tissues by IHC.

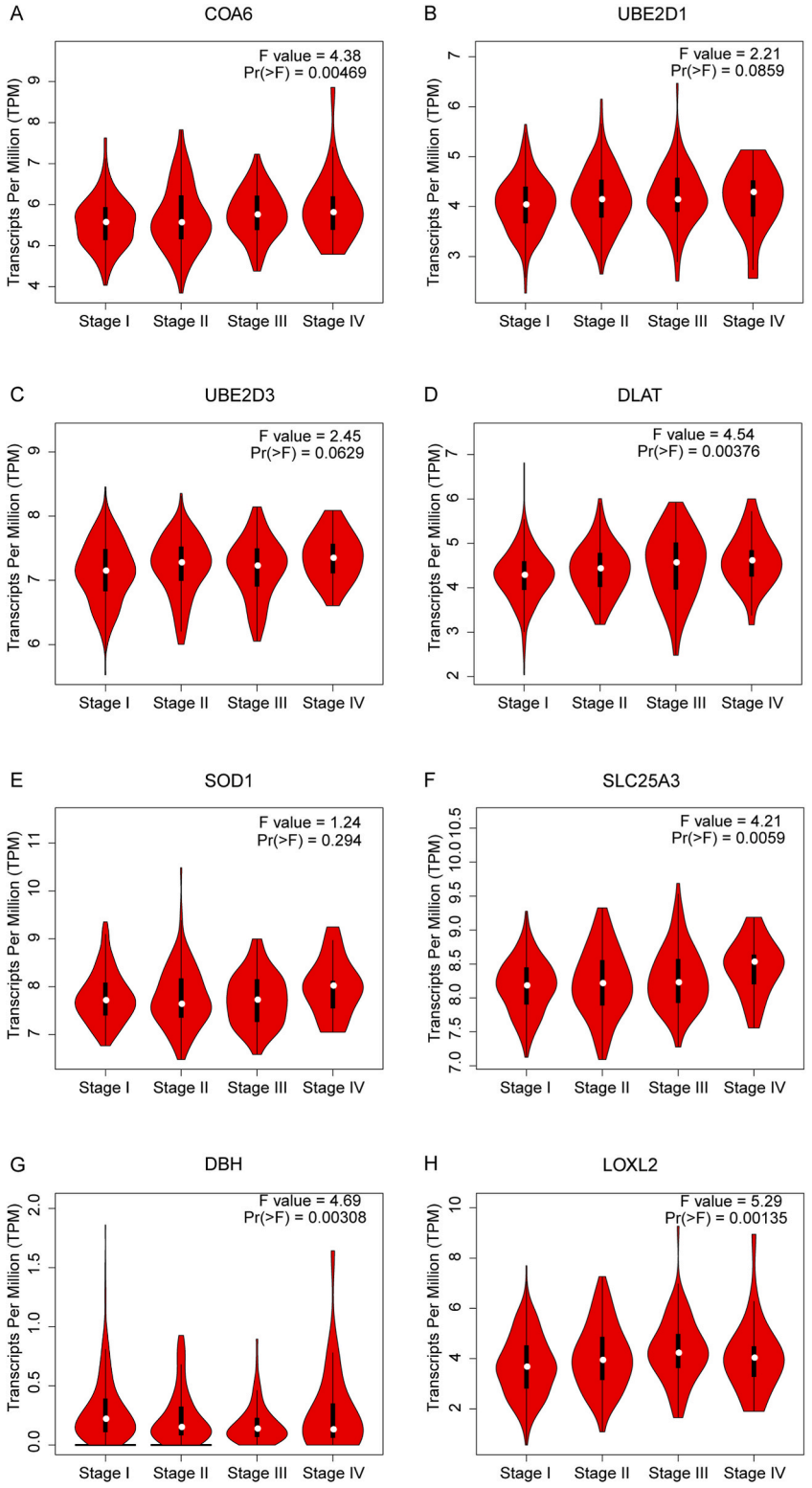

Fig. 4. CRG expression in relation to individual cancer stages. (A) COA6, (B) UBE2D1, (C) UBE2D3, (D) DLAT, (E) SOD1, (F) SLC25A3, (G) DBH, and (H) LOXL2 showed different association with clinical stages in LUAD.

According to the IHC staining results, the protein level of COA6, UBE2D1, DLAT, SLC25A3 and LOXL2 was increased, while DBH without significant difference in LUAD tissues than that in paracancerous tissues (Fig. 3I-T). HPA database showed that the protein expression of COA6, DLAT and UBE2D1 in LUAD tissues was higher than that in normal lung tissues (Supplementary Figs. 2A–C). However, protein level of UBE2D3 in the LUAD tissue sample was not detected (Supplementary Fig. 2D).

3.5. CRG expression in relation to individual cancer stages

GEPIA database was used to explore the correlation between CRG expression and clinicopathological features. The results showed that COA6 ($P = 0.00469$), DLAT ($P = 0.00376$), SLC25A3 ($P = 0.0059$), DBH ($P = 0.00308$), and LOXL2 ($P = 0.00135$) were all strongly associated with the clinicopathological stages in LUAD (Fig. 4A–D, F-H). The expression of UBE2D1 ($P = 0.0859$), UBE2D3 ($P = 0.0629$) and SOD1 ($P = 0.294$) indicated no obvious association with stages of LUAD (Fig. 4B, C, E). Thus, with the disease progresses, the expression levels of COA6, DLAT, SLC25A3, DBH and LOXL2 tend to increase as demonstrated by TGCA database, which indicates that they might play important roles in the development of LUAD.

3.6. Prognostic implication of CRGs in LUAD

Kaplan-Meier plotter was utilized to explore the prognostic value of CRGs in LUAD. We conducted analyses of the relationship between CRG expression and OS as well as recurrence-free survival (RFS) of LUAD. The results showed that the high expression of COA6 (HR = 1.78, $P = 0.00011$), UBE2D1 (HR = 1.47, $P = 0.011$), DLAT (HR = 1.36, $P = 0.048$), SLC25A3 (HR = 1.49, $P = 0.0099$), and LOXL2 (HR = 1.83, $P = 3.7e-05$) was strongly related to poor OS in LUAD patients, while the high expression of DBH (HR = 0.6, $P = 0.00093$) was linked to favorable OS (Fig. 5A–H). As for the RFS of LUAD patients, elevated expression of LOXL2 (HR = 1.66, $P = 0.027$) was associated with inferior RFS, whereas high expression of SLC25A3 (HR = 0.55, $P = 0.0061$) was correlated to favorable RFS, without significance of COA6 (HR = 0.77, $P = 0.26$), UBE2D1 (HR = 1.42, $P = 0.11$), UBE2D3 (HR = 1.4, $P = 0.13$), DLAT (HR = 0.64, $P = 0.084$), SOD1 (HR = 1.19, $P = 0.43$), and DBH (HR = 1.46, $P = 0.13$) (Supplementary Figs. 3A–H). Thus, SLC25A and LOXL2 are closely related to the poor prognosis of patients and might be used as biomarkers to predict the survival time of patients with LUAD. Based on the aforementioned findings, this study chose SLC25A3 and LOXL2 for further investigation.

3.7. Immune infiltration analysis of SLC25A3 and LOXL2 in LUAD

To investigate the immune cell infiltration of CRGs in LUAD, MCP-counter, ssGSEA and TIMER were applied. TCGA samples were divided into two groups based on SLC25A3 mRNA expression, MCP-counter results showed that $CD8^+$ T cell, T cell, B cell, and myeloid

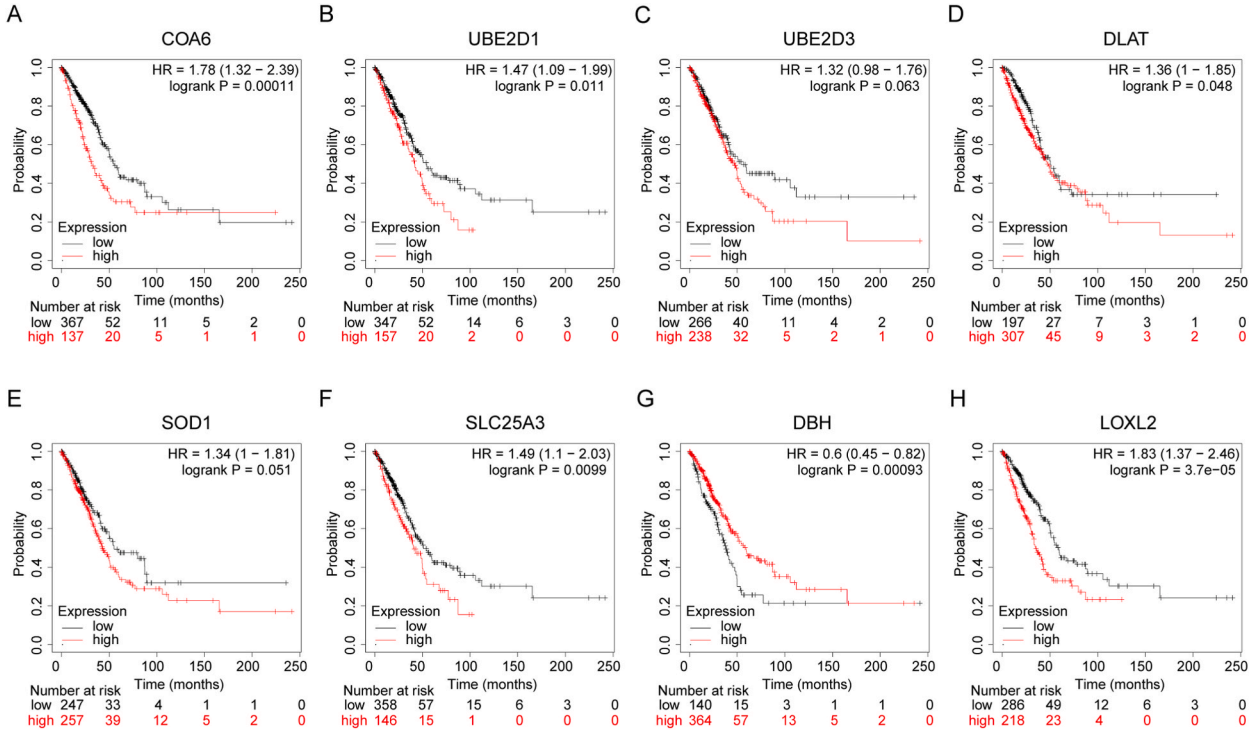

Fig. 5. Prognostic significance of CRGs in LUAD. The relationship between (A) COA6, (B) UBE2D1, (C) UBE2D3, (D) DLAT, (E) SOD1, (F) SLC25A3, (G) DBH, and (H) LOXL2 and OS of LUAD patients.

dendritic cell (DC) are the significantly different immune cell types infiltrated between SLC25A3 high and low expression samples (Fig. 6A). The expression of SLC25A3 was strongly negatively correlated with B cells, TFH, T cells, pDC, Th1 cells, Cytotoxic cells, Treg, Tem, Macrophages, NK CD56bright cells and iDC, with positive correlation with Th2 cells and Tgd by ssGSEA (Fig. 6B and Supplementary Fig. 4). MCP-counter analysis showed an association between LOXL2 expression and Neutrophil, Myeloid DC, Monocyte and Macrophage/Monocyte (Fig. 6C). The expression of LOXL2 was strongly positively associated with Th2 cells, Neutrophils, NK

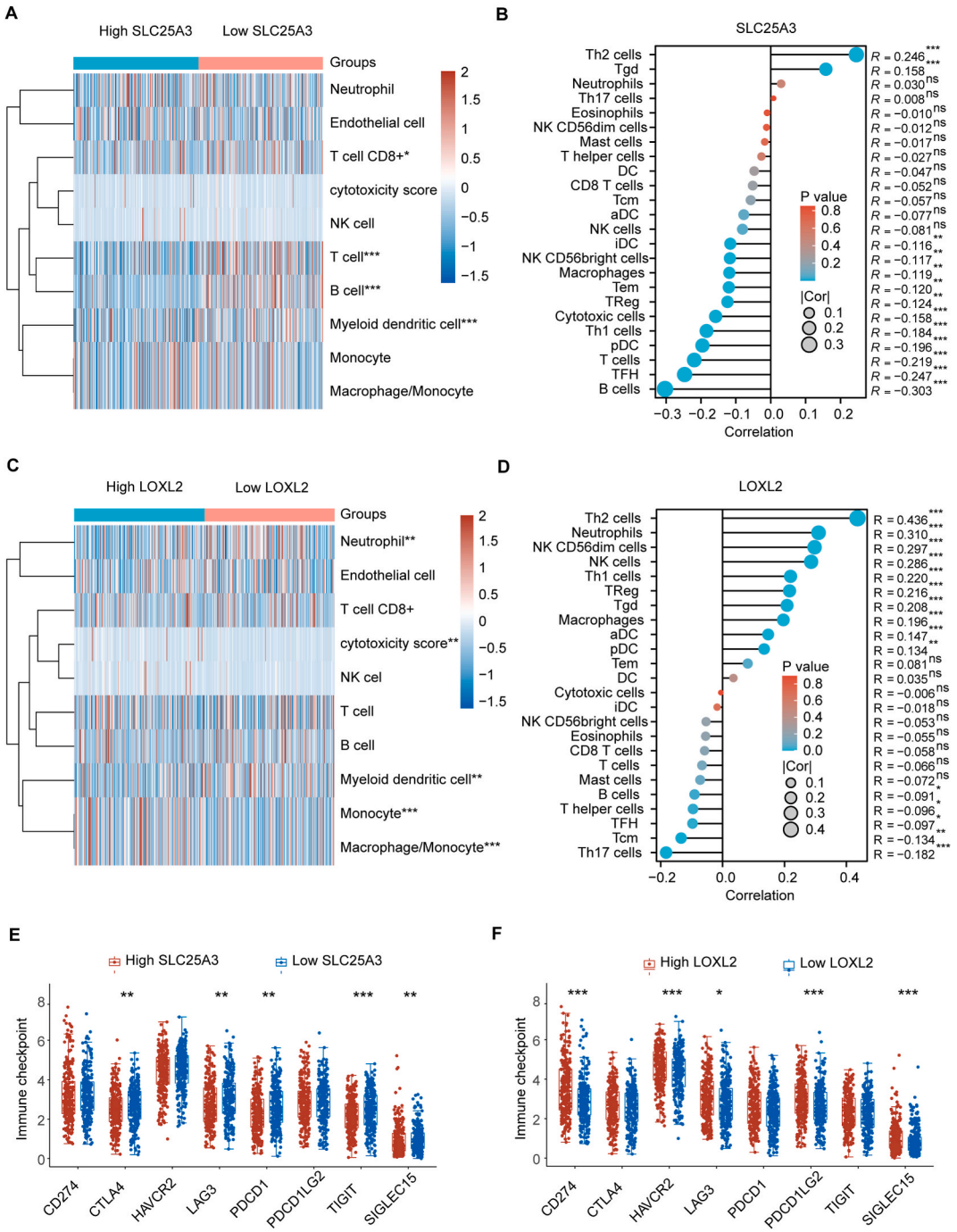

Fig. 6. The correlation between SLC25A3, LOXL2 expression and immune cells infiltration, and immune checkpoints in LUAD. The association between SLC25A3 (A) and LOXL2 (C) expression and immune cells infiltration in LUAD based on MCP-counter. Lollipop diagram displaying the correlation between SLC25A3 (B) and LOXL2 (D) expression and 24 immune cells infiltration by ssGSEA. Box plot comparing immune checkpoints expression between $SLC25A3^{high}$ and $SLC25A3^{low}$ groups (E), and $LOXL2^{high}$ and $LOXL2^{low}$ groups (F) in LUAD patients. $^{*}P < 0.05$, $^{**}P < 0.01$, $^{***}P < 0.001$.

CD56dim cells, NK cells, Th1 cells, Treg, Tgd, Macrophages, aDC and pDC, with negative relation to Th17 cells, Tcm, TFH, T helper cells and B cells by ssGSEA (Fig. 6D and Supplementary Fig. 5).

Meanwhile, we searched the TIMER database for the correlation between the infiltration of B cells, $CD8^+$ T cells, $CD4^+$ T cells, neutrophils, macrophages, DCs, and the expression of SLC25A3, LOXL2, respectively. The expression of SLC25A3 was negatively correlated with B cells (Partial cor = -0.027, $P = 5.33e\text{-}07$), $CD4^+$ T cells (Partial cor = -0.184, $P = 4.60e\text{-}05$), and DCs (Partial cor = -0.1, $P = 2.69e\text{-}02$), but positively related with $CD8^+$ T cells (Partial cor = 0.099, $P = 2.91e\text{-}02$). And the expression of LOXL2 was negatively linked to B cells (Partial cor = -0.209, $P = 3.71e\text{-}06$) and positively correlated with neutrophils (Partial cor = 0.219, $P = 1.22e\text{-}06$) (Supplementary Fig. 6A). In addition, compared to normal tissues, SLC25A3, LOXL2, and their different copy states had a certain effect on immune infiltration. The arm-level gain of SLC25A3 showed significant differences in B cell, $CD4^+$ T cell and macrophage infiltration, whereas deep deletion, arm-level deletion, and arm-level gain of LOXL2 revealed considerable differences in $CD4^+$ T cell, macrophage and DC infiltration (Supplementary Figs. 6B–C).

3.8. Immune checkpoints analysis of SLC25A3 and LOXL2 in LUAD

The correlation of SLC25A3, LOXL2 and the major eight immune checkpoint genes were performed. The expression of SLC25A3 showed negative relation to CTLA4 ($R = -0.204$, $P < 0.001$), LAG3 ($R = -0.117$, $P = 0.007$), PDCD1 ($R = -0.135$, $P = 0.002$), TIGIT ($R = -0.212$, $P < 0.001$). SIGLEC15 ($R = -0.149$, $P < 0.001$) (Fig. 6E). However, there presented a consistently positive correlation of LOXL2 expression with the five immune checkpoint genes, CD274 ($R = 0.273$, $P < 0.001$), HAVCR2 ($R = 0.222$, $P < 0.001$), LAG3 ($R = 0.155$, $P < 0.001$), PDCD1LG2($R = 0.248$, $P < 0.001$), SIGLEC15 ($R = 0.170$, $P < 0.001$) (Fig. 6F).

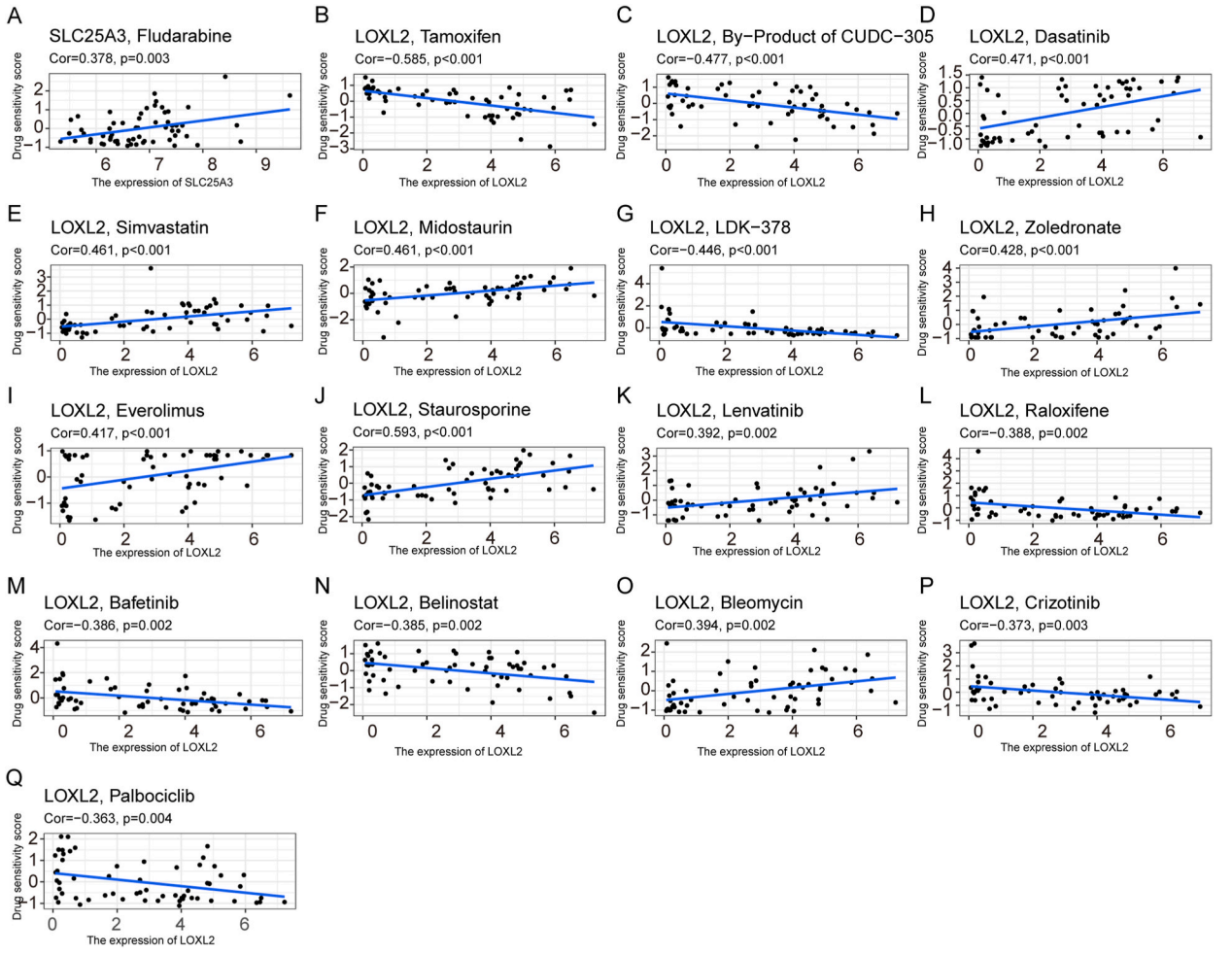

Fig. 7. The drug sensitivity analysis. (A) Correlation of SLC25A3 with fludarabine. Correlation of LOXL2 with Tamoxifen (B), by-product of CUDC-305 (C), Dasatinib (D), Simvastatin (E), Midostaurin (F), LDK-378 (G), Zoledronate (H), Everolimus (I), Staurosporine (J), Lenvatinib (K), Raloxifene (L), Bafetinib (M), Belinostat (N), Bleomycin (O), Crizotinib (P), and Palbociclib (Q).

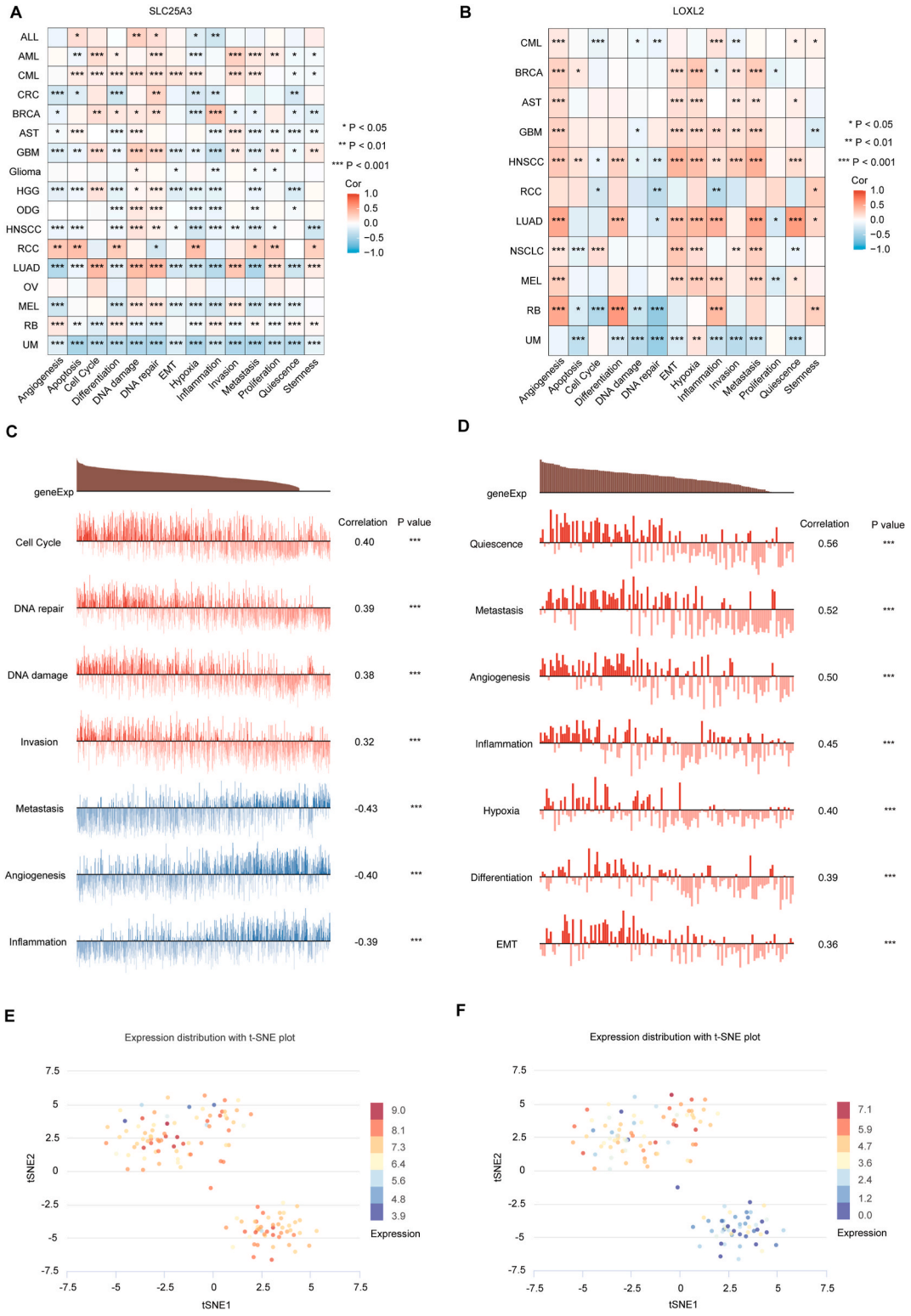

Fig. 8. The expression and function states of SLC25A3 and LOXL2 at single-cell level. (A–D) CancerSEA was used to investigate the connection between SLC25A3 and LOXL2 expression and various functional states in tumors at single-cell level. *$P < 0.05$, **$P < 0.01$, ***$P < 0.001$. (E–F) T-SNE diagrams displayed the SLC25A3 and LOXL2 expression patterns at single cells from LUAD.

3.9. Drug sensitivity analysis of SLC25A3 and LOXL2 in LUAD

Subsequently, we carried out a drug sensitivity analysis. The results showed that SLC25A3 was positively correlated with fludarabine (Fig. 7A). LOXL2 was positively correlated with Dasatinib, Simvastatin, Midostaurin, Zoledronate, Everolimus, Staurosporine, Lenvatinib and Bleomycin (Fig. 7D–F, H–K, O), while negatively correlated with Tamoxifen, a by-product of CUDC-305, LDK-378, Raloxifene, Bafetinib, Belinostat, Crizotinib, and Palbociclib (Fig. 7B, C, G, L-N, P, Q).

3.10. The expression and function states of SLC25A3 and LOXL2 at single-cell level

In LUAD, the expression of SLC25A3 was positively associated with cell cycle, DNA damage, DNA repair and invasion, while negatively related to angiogenesis, apoptosis, differentiation, EMT (Epithelial-mesenchymal transition), hypoxia, inflammation, metastasis and quiescence (Fig. 8A). LOXL2 had a positive relationship with almost all tumor biological behaviors, such as angiogenesis, differentiation, EMT, hypoxia, inflammation, metastasis, quiescence and stemness (Fig. 8B).

In addition, the significant correlation between the expression of SLC25A3 and cell cycle ($R = 0.40$, $P < 0.001$), DNA repair ($R = 0.39$, $P < 0.001$), DNA damage ($R = 0.38$, $P < 0.001$), invasion ($R = 0.32$, $P < 0.001$), metastasis ($R = -0.43$, $P < 0.001$), angiogenesis ($R = -0.40$, $P < 0.001$) and inflammation ($R = -0.39$, $P < 0.001$) was displayed (Fig. 8C). The significant positive association between the expression of LOXL2 and quiescence ($R = 0.56$, $P < 0.001$), metastasis ($R = 0.52$, $P < 0.001$), angiogenesis ($R = 0.50$, $P < 0.001$), inflammation ($R = 0.45$, $P < 0.001$), hypoxia ($R = 0.40$, $P < 0.001$), differentiation ($R = 0.39$, $P < 0.001$), and EMT ($R = 0.36$, $P < 0.001$) was illustrated (Fig. 8D). Moreover, the expression profiles of SLC25A3 and LOXL2 were shown at single-cell level from LUAD by T-SNE diagrams (Fig. 8E and F).

4. Discussion

Recent years, emerging studies have shown that cuproptosis plays an important role in the occurrence, progression and treatment of human tumors [29]. Among all human cancers, lung cancer is one of the most malignant types with the highest morbidity and fatality rates globally. The OS of patients is far from satisfaction, though the prognoses have greatly improved by recent treatment advancements. Currently, it is still unclear how lung cancer initiates or develops. The inferior prognosis and high rate of recurrence make it urgent to explore the underlying mechanism of occurrence and development. Also, it is necessary to discover potential biomarkers related to prognosis.

The maintenance of cell life cycle, or cell death, is crucial to the expansion and maturation of organisms. There exist several types of cell death, including cell necrosis, apoptosis, pyroptosis, and ferroptosis. In addition, Tsvetkov et al. proposed a brand-new programmed cell death named cuproptosis, distinct from the above mechanisms of cell death. It is a novel kind of controlled and copper-dependent form of death that is quite similar to mitochondrial respiration. As we are all aware, copper is a common metal element with redox activity and a vital mineral for all living things. During most of the lifetime, intestinal cells absorb copper from meals. Adults require 0.9 mg of copper per day [30]. If the body absorbs too much Cu^{2+}, it will increase the production of hydroxyl radicals, the level of reactive oxygen species (ROS) in cells, and enhance lipid peroxidation, leading to oxidative stress and apoptosis. The amount of copper in the body maintains a dynamic balance, and when the balance is disrupted, it will produce cytotoxicity and induce cell death by a variety of pathways [31,32]. According to the recent study, copper metabolic disorders are becoming more and more common, particularly in the field of cancer [33].

We sorted out 41 CRGs by consulting the literature. There are 32 genes differentially expressed in LUAD. Among them, MDC1 is a key protein involved in double-stranded DNA damage repair, induces its expression through antioxidant 1 copper chaperone (ATOX1), which in turn promotes the drug resistance of cancer cells and the repair of DNA damage [34]. Elesclomol is a tiny molecule that can transport copper ions through cell membranes and kill particular cancer cells that are drug-resistant. Research shows that elesclomol directly targets FDX1, coding for a reductase turning Cu^{2+} into Cu^{+} [35]. LIAS is involved in protein lipid acylation, while DLAT, MTF1, GLS, and CDKN2A are related to the formation of the pyruvate dehydrogenase complex [10]. The ubiquitin-conjugating enzyme E2D1 (UBE2D1), a member of the UBE2D family, has been found to play a role in certain important carcinogenic pathways. UBE2D1 can reduce the ubiquitin level of decapentaplegic homolog 4 (SMAD4). Through the transforming growth factor β (TGF-β)/SMAD4 pathway, silencing UBE2D4 can inhibit the proliferation and migration of gastric cancer cells [36]. It has been reported that phosphoinositide-dependent protein kinase-1 (PDK1) can bind to copper and activate its downstream substrate AKT to promote tumorigenesis [37]. Superoxide dismutase-1 (SOD1) is a major antioxidant and plays a carcinogenic role in many cancers. SOD1 expression is up-regulated in NSCLC cells and tissues; inhibition of SOD1 can induce NSCLC cell arrest in G1 phase and promote apoptosis [38]. SLC25A3, which encodes a mitochondrial phosphate carrier, is involved in the transport of phosphate across the mitochondrial inner membrane, a process critical for cellular energy metabolism. Its function in cancer development and progression is multifaceted and can be influenced by several factors, such as genetic alterations and environmental contexts [39]. Research has indicated that alterations in SLC25A3 can lead to changes in cellular metabolism, which is often deregulated in cancer cells. For instance, changes in the expression or function of SLC25A3 could potentially affect the ability of cells to produce energy through oxidative phosphorylation, impacting their proliferation and survival [40]. Moreover, the mitochondrial phosphate carrier has been implicated in the regulation of the mitochondrial permeability transition pore (mPTP), which can influence cell death pathways and function as a potential target in cancer therapy [41]. Lysyl oxidase-like 2 (LOXL2) is a member of the scavenger-receptor cysteine-rich (SRCR) family that carries LOX, which is related to histone binding and chromatin modification. Studies have demonstrated that LOXL2 is a tumor suppressor, and low expression of LOXL2 can promote the progress of uterine cancer and inhibit the efficacy of

anti-PD-1 therapy [42]. Thus, CRGs may play an important role in the occurrence and development of several types of tumors, but with few studies in LUAD.

In our present study, enrichment analysis showed that cuproptosis-related genes are mainly related to life activities such as copper ion transport, cellular copper ion homeostasis, copper ion homeostasis, TCA cycle, and central carbon metabolism in cancer. HPA database showed that COA6, DLAT and UBE2D1 were highly expressed in LUAD tissues, while UBE2D3 was low. We investigated the expression of CRG mRNA and protein in LUAD using qRT-PCR and Western blots for clinical sample verification to strengthen the validity of the above results. Similarly, CRGs were differentially expressed in LUAD, and there revealed a strong correlation between SLC25A3, LOXL2, and the prognosis of LUAD patients. However, there were discrepancies regarding the mRNA expression levels of CRGs in GSE101929 and TCGA, our IHC results of CRGs and HPA data. The potential reasons for these observed discrepancies were mainly differences in sample preparation, antibody specificity, data processing methods and the limited numbers of our collected LUAD samples. Thus, it is urgent for further research to resolve these inconsistencies and to provide a more definitive understanding of the function of CRGs in cancer.

Tumor treatment has recently concentrated on tumor immune escape. The microenvironment of tumor tissue is home to a variety of immune cells, which control the behavior of other cells and have direct or indirect effects on the tumor microenvironment (TME). Immune cell therapy offers a wide range of potential applications in LUAD treatment. We discovered that the expression of SLC25A3 and LOXL2 connected to the invasion of immune cells, such as Th2 cells, NK cells, and B cells, which could provide fresh perspectives on immunotherapy for LUAD. Additionally, it was observed that there existed certain differences in the immune infiltration results between the MCP counter and TIMER. It is speculated that the differences in the algorithms and data sources might explain the potential reasons in light of these differences. To further validate our results, we have to perform additional analyses using other independent datasets and databases, which could help to cross-verify the findings and strengthens the robustness of the conclusions.

The understanding of the regulation of immune checkpoint molecules has changed the traditional tumor therapy. Immune checkpoint molecules are widely available and can be employed for medication. The immunological features of SLC25A3 and LOXL2 in LUAD were thoroughly explored in this work, including immune cell infiltration, immune checkpoint gene expression, and single cell analysis in the TME. The expression of SLC25A3 showed negative relation to CTLA4, LAG3, PDCD1 and TIGIT. However, LOXL2 presented a consistently positive correlation with CD274, HAVCR2, LAG3, PDCD1LG2 and SIGLEC15. One of the main barriers to this treatment is lack of diagnostic indicators to pinpoint patients who will react to immune checkpoint blocking drugs. We found that SLC25A3 and LOXL2 could reliably predict the immunological checkpoints' expression status in LUAD. This provides important clues for subsequent tumor immunotherapy in clinical practice.

The drug sensitivity analysis results for SLC25A3 and LOXL2 could provide valuable insights into the potential therapeutic targets for LUAD treatment. High expression levels of these genes may suggest a significant role in the proliferation and survival of LUAD cells. Consequently, drugs that target these genes could potentially disrupt the cancer cells' growth and spread, offering a new avenue for targeted therapy. Besides, the single-cell sequencing data for SLC25A3 and LOXL2 can reveal the heterogeneity of LUAD at the single cell level. By examining the expression patterns of these genes in individual cells, we can identify the different functional states of cells in types of tumors, especially LUAD in our context. This information is crucial for understanding the complexity of LUAD and could guide the development of more personalized treatment strategies.

Nevertheless, our research still has certain limitations, despite the aforementioned findings. There is an urgent need to further evaluate the function of CRGs at the cellular and molecular level via *in vitro* and *in vivo* experiments. Besides, we will explore further into CRGs' role in immunotherapy and offer novel ideas for the clinical treatment of LUAD.

5. Conclusion

In our present research, we analyzed the expression of CRGs in LUAD and screened out prognosis-related genes. Future advancements in the identification and treatment of tumors may be made possible by CRGs, which are anticipated to be viable targets for LUAD therapy. Additionally, SLC25A3 and LOXL2 could predict LUAD patients' responses to immunotherapy, which offers crucial clues in therapeutic manipulation.

Declarations

Data availability statement

All datasets are publicly available. TCGA dataset is available via the following link: https://portal.gdc.cancer.gov/. The GEO database is available via the following link: https://www.ncbi.nlm.nih.gov/geo/. The Human Protein Atlas (HPA) database is available in the public domain via the following link: www.proteinatlas.org. Gene Expression Profiling Interactive Analysis (GEPIA) is available via http://gepia.cancer-pku.cn/index.html. The Kaplan-Meier plotter is publicly available via https://kmplot.com/analysis. Tumor IMmune Estimation Resource (TIMER) is an online tool available in the public domain via https://cistrome.shinyapps.io/timer/. CancerSEA is available via the following link: http://biocc.hrbmu.edu.cn/CancerSEA/.

Ethics statement

This study was approved by the ethics committee of the Affiliated Hospital of Jining Medical University, in accordance with the principles of the Declaration of Helsinki. There are no human participants in this study.

Funding

This work was supported by the National Natural Science Foundation of China (81800182, 81802290).

CRediT authorship contribution statement

Liming Zhang: Writing – original draft, Software, Methodology, Investigation, Formal analysis. **Shaoqiang Wang:** Validation, Supervision, Resources, Funding acquisition, Data curation. **Lina Wang:** Writing – review & editing, Project administration, Funding acquisition, Conceptualization.

Declaration of competing interest

The authors declare the following financial interests/personal relationships which may be considered as potential competing interests:

Lina Wang reports financial support was provided by National Natural Science Foundation of China. Shaoqiang Wang reports financial support was provided by National Natural Science Foundation of China. If there are other authors, they declare that they have no known competing financial interests or personal relationships that could have appeared to influence the work reported in this paper.

Appendix A. Supplementary data

Supplementary data to this article can be found online at https://doi.org/10.1016/j.heliyon.2024.e30446.

References

[1] H. Sung, J. Ferlay, R.L. Siegel, M. Laversanne, I. Soerjomataram, A. Jemal, F. Bray, Global cancer statistics 2020: GLOBOCAN estimates of incidence and mortality worldwide for 36 cancers in 185 countries, CA A Cancer J. Clin. 71 (2021) 209–249.
[2] C. Zhang, N.B. Leighl, Y.L. Wu, W.Z. Zhong, Emerging therapies for non-small cell lung cancer, J. Hematol. Oncol. 12 (2019) 45.
[3] K.C. Arbour, G.J. Riely, Systemic therapy for locally advanced and metastatic non-small cell lung cancer: a review, JAMA 322 (2019) 764–774.
[4] Y. Li, M.A. Trush, DNA damage resulting from the oxidation of hydroquinone by copper: role for a Cu(II)/Cu(I) redox cycle and reactive oxygen generation, Carcinogenesis 14 (1993) 1303–1311.
[5] T. Atakul, S.O. Altinkaya, B.I. Abas, C. Yenisey, Serum copper and zinc levels in patients with endometrial cancer, Biol. Trace Elem. Res. 195 (2020) 46–54.
[6] Y. Feng, J.W. Zeng, Q. Ma, S. Zhang, J. Tang, J.F. Feng, Serum copper and zinc levels in breast cancer: a meta-analysis, J. Trace Elem. Med. Biol. 62 (2020) 126629.
[7] V. Pavithra, T.G. Sathisha, K. Kasturi, D.S. Mallika, S.J. Amos, S. Ragunatha, Serum levels of metal ions in female patients with breast cancer, J. Clin. Diagn. Res. 9 (2015) BC25–c27.
[8] L. Huang, R. Shen, L. Huang, J. Yu, H. Rong, Association between serum copper and heart failure: a meta-analysis, Asia Pac. J. Clin. Nutr. 28 (2019) 761–769.
[9] V. Oliveri, Selective targeting of cancer cells by copper ionophores: an overview, Front. Mol. Biosci. 9 (2022) 841814.
[10] P. Tsvetkov, S. Coy, B. Petrova, M. Dreishpoon, A. Verma, M. Abdusamad, J. Rossen, L. Joesch-Cohen, R. Humeidi, R.D. Spangler, J.K. Eaton, E. Frenkel, M. Kocak, S.M. Corsello, S. Lutsenko, N. Kanarek, S. Santagata, T.R. Golub, Copper induces cell death by targeting lipoylated TCA cycle proteins, Science 375 (2022) 1254–1261.
[11] G. Pistritto, D. Trisciuoglio, C. Ceci, A. Garufi, G. D'Orazi, Apoptosis as anticancer mechanism: function and dysfunction of its modulators and targeted therapeutic strategies, Aging (Albany NY) 8 (2016) 603–619.
[12] J. Shi, W. Gao, F. Shao, Pyroptosis: gasdermin-mediated programmed necrotic cell death, Trends Biochem. Sci. 42 (2017) 245–254.
[13] S.J. Dixon, K.M. Lemberg, M.R. Lamprecht, R. Skouta, E.M. Zaitsev, C.E. Gleason, D.N. Patel, A.J. Bauer, A.M. Cantley, W.S. Yang, B. Morrison 3rd, B. R. Stockwell, Ferroptosis: an iron-dependent form of nonapoptotic cell death, Cell 149 (2012) 1060–1072.
[14] K. Tomczak, P. Czerwińska, M. Wiznerowicz, The Cancer Genome Atlas (TCGA): an immeasurable source of knowledge, Contemp. Oncol. 19 (2015) A68–A77.
[15] T. Barrett, S.E. Wilhite, P. Ledoux, C. Evangelista, I.F. Kim, M. Tomashevsky, K.A. Marshall, K.H. Phillippy, P.M. Sherman, M. Holko, A. Yefanov, H. Lee, N. Zhang, C.L. Robertson, N. Serova, S. Davis, A. Soboleva, NCBI GEO: archive for functional genomics data sets–update, Nucleic Acids Res. 41 (2013) D991–D995.
[16] S. Cattley, J.W. Arthur, BioManager: the use of a bioinformatics web application as a teaching tool in undergraduate bioinformatics training, Briefings Bioinf. 8 (2007) 457–465.
[17] A. Mayakonda, D.C. Lin, Y. Assenov, C. Plass, H.P. Koeffler, Maftools: efficient and comprehensive analysis of somatic variants in cancer, Genome Res. 28 (2018) 1747–1756.
[18] G. Yu, L.G. Wang, Y. Han, Q.Y. He, clusterProfiler: an R package for comparing biological themes among gene clusters, OMICS 16 (2012) 284–287.
[19] S. Navani, Manual evaluation of tissue microarrays in a high-throughput research project: the contribution of Indian surgical pathology to the Human Protein Atlas (HPA) project, Proteomics 16 (2016) 1266–1270.
[20] Z. Tang, C. Li, B. Kang, G. Gao, C. Li, Z. Zhang, GEPIA: a web server for cancer and normal gene expression profiling and interactive analyses, Nucleic Acids Res. 45 (2017) W98–w102.
[21] A. Lánczky, B. Győrffy, Web-based survival analysis tool tailored for medical research (KMplot): development and implementation, J. Med. Internet Res. 23 (2021) e27633.
[22] T. Li, J. Fan, B. Wang, N. Traugh, Q. Chen, J.S. Liu, B. Li, X.S. Liu, TIMER: a web server for comprehensive analysis of tumor-infiltrating immune cells, Cancer Res. 77 (2017) e108–e110.
[23] H. Yuan, M. Yan, G. Zhang, W. Liu, C. Deng, G. Liao, L. Xu, T. Luo, H. Yan, Z. Long, A. Shi, T. Zhao, Y. Xiao, X. Li, CancerSEA: a cancer single-cell state atlas, Nucleic Acids Res. 47 (2018) D900–D908.
[24] L. Li, W. Yao, S. Yan, X. Dong, Z. Lv, Q. Jing, Q. Wang, B. Ma, C. Hao, D. Xue, D. Wang, Pan-cancer analysis of prognostic and immune infiltrates for CXCs, Cancers 13 (2021).
[25] J. He, H. Ding, H. Li, Z. Pan, Q. Chen, Intra-tumoral expression of SLC7A11 is associated with immune microenvironment, drug resistance, and prognosis in cancers: a pan-cancer analysis, Front. Genet. 12 (2021) 770857.

[26] Y. Ye, Q. Dai, H. Qi, A novel defined pyroptosis-related gene signature for predicting the prognosis of ovarian cancer, Cell Death Dis. 7 (2021) 71.
[27] R. Karki, T.D. Kanneganti, Diverging inflammasome signals in tumorigenesis and potential targeting, Nat. Rev. Cancer 19 (2019) 197–214.
[28] S.M. Man, T.D. Kanneganti, Regulation of inflammasome activation, Immunol. Rev. 265 (2015) 6–21.
[29] Y. Jiang, Z. Huo, X. Qi, T. Zuo, Z. Wu, Copper-induced tumor cell death mechanisms and antitumor theragnostic applications of copper complexes, Nanomedicine (Lond) 17 (2022) 303–324.
[30] Food Labeling, Revision of the nutrition and supplement facts labels. Final rule, Fed. Regist. 81 (2016) 33741–33999.
[31] S. Osawa, K. Kitanishi, M. Kiuchi, M. Shimonaka, H. Otsuka, Accelerated redox reaction of hydrogen peroxide by employing locally concentrated state of copper catalysts on polymer chain, Macromol. Rapid Commun. 42 (2021) e2100274.
[32] B. Halliwell, S. Chirico, Lipid peroxidation: its mechanism, measurement, and significance, Am. J. Clin. Nutr. 57 (1993) 715S–724S. ; discussion 724S-725S.
[33] E.J. Ge, A.I. Bush, A. Casini, P.A. Cobine, J.R. Cross, G.M. DeNicola, Q.P. Dou, K.J. Franz, V.M. Gohil, S. Gupta, S.G. Kaler, S. Lutsenko, V. Mittal, M.J. Petris, R. Polishchuk, M. Ralle, M.L. Schilsky, N.K. Tonks, L.T. Vahdat, L. Van Aelst, D. Xi, P. Yuan, D.C. Brady, C.J. Chang, Connecting copper and cancer: from transition metal signalling to metalloplasia, Nat. Rev. Cancer 22 (2022) 102–113.
[34] J. Jin, M. Ma, S. Shi, J. Wang, P. Xiao, H.F. Yu, C. Zhang, Q. Guo, Z. Yu, Z. Lou, C.B. Teng, Copper enhances genotoxic drug resistance via ATOX1 activated DNA damage repair, Cancer Lett. 536 (2022) 215651.
[35] P. Tsvetkov, A. Detappe, K. Cai, H.R. Keys, Z. Brune, W. Ying, P. Thiru, M. Reidy, G. Kugener, J. Rossen, M. Kocak, N. Kory, A. Tsherniak, S. Santagata, L. Whitesell, I.M. Ghobrial, J.L. Markley, S. Lindquist, T.R. Golub, Mitochondrial metabolism promotes adaptation to proteotoxic stress, Nat. Chem. Biol. 15 (2019) 681–689.
[36] H. Xie, Y. He, Y. Wu, Q. Lu, Silencing of UBE2D1 inhibited cell migration in gastric cancer, decreasing ubiquitination of SMAD4, Infect. Agents Cancer 16 (2021) 63.
[37] J. Guo, J. Cheng, N. Zheng, X. Zhang, X. Dai, L. Zhang, C. Hu, X. Wu, Q. Jiang, D. Wu, H. Okada, P.P. Pandolfi, W. Wei, Copper promotes tumorigenesis by activating the PDK1-AKT oncogenic pathway in a copper transporter 1 dependent manner, Adv. Sci. 8 (2021) e2004303.
[38] S. Liu, B. Li, J. Xu, S. Hu, N. Zhan, H. Wang, C. Gao, J. Li, X. Xu, SOD1 promotes cell proliferation and metastasis in non-small cell lung cancer via an miR-409-3p/SOD1/SETDB1 epigenetic regulatory feedforward loop, Front. Cell Dev. Biol. 8 (2020) 213.
[39] P. Jiang, W. Du, A. Mancuso, K.E. Wellen, X. Yang, Reciprocal regulation of p53 and malic enzymes modulates metabolism and senescence, Nature 493 (2013) 689–693.
[40] J.J. Ruprecht, E.R.S. Kunji, The SLC25 mitochondrial carrier family: structure and mechanism, Trends Biochem. Sci. 45 (2020) 244–258.
[41] A. Boulet, K.E. Vest, M.K. Maynard, M.G. Gammon, A.C. Russell, A.T. Mathews, S.E. Cole, X. Zhu, C.B. Phillips, J.Q. Kwong, S.C. Dodani, S.C. Leary, P.A. Cobine, The mammalian phosphate carrier SLC25A3 is a mitochondrial copper transporter required for cytochrome c oxidase biogenesis, J. Biol. Chem. 293 (2018) 1887–1896.
[42] X. Lu, D.E. Xin, J.K. Du, Q.C. Zou, Q. Wu, Y.S. Zhang, W. Deng, J. Yue, X.S. Fan, Y. Zeng, X. Cheng, X. Li, Z. Hou, M. Mohan, T.C. Zhao, X. Lu, Z. Chang, L.Y. Xu, Y. Sun, X. Zu, Y. Zhang, Y.E. Chin, Loss of LOXL2 promotes uterine hypertrophy and tumor progression by enhancing H3K36ac-dependent gene expression, Cancer Res 82 (2022) 4400–4413.